PHYSICAL REVIEW C **72**, 061002(R) (2005)

Evidence of three-body force effects in neutron-deuteron scattering at 95 MeV

P. Mermod, J. Blomgren,* A. Hildebrand, C. Johansson, J. Klug, M. Österlund, S. Pomp, and U. Tippawan
Department of Neutron Research, Uppsala University, Box 525, S-75120 Uppsala, Sweden

B. Bergenwall
Department of Neutron Research, Uppsala University, Box 525, S-75120 Uppsala, Sweden and Department of Radiation Sciences, Uppsala University, Sweden

L. Nilsson
Department of Neutron Research, Uppsala University, Box 525, S-75120 Uppsala, Sweden and The Svedberg Laboratory, Uppsala University, Sweden

N. Olsson
Department of Neutron Research, Uppsala University, Box 525, S-75120 Uppsala, Sweden and Swedish Defence Research Agency (FOI), Stockholm, Sweden

O. Jonsson, A. Prokofiev, and P.-U. Renberg
The Svedberg Laboratory, Uppsala University, Sweden

P. Nadel-Turonski
Department of Radiation Sciences, Uppsala University, Sweden and George Washington University, Washington, D.C., USA

Y. Maeda, H. Sakai, and A. Tamii
Department of Physics, University of Tokyo, Japan
(Received 17 June 2005; published 30 December 2005)

Recently, we have reported a measurement of the neutron-deuteron elastic scattering differential cross section at 95 MeV. In the present work, the previous results are confirmed with an independent measurement performed with another setup. The new data cover the full angular distribution by combining neutron detection and deuteron detection, and have an unprecedented precision in the region of the cross-section minimum, where three-nucleon forces are expected to be significant. The effect already identified in the previous measurement is clearly seen in the present data, which agree well with theoretical descriptions including three-nucleon forces.

DOI: 10.1103/PhysRevC.72.061002 PACS number(s): 21.45.+v, 25.10.+s, 25.40.Dn, 28.20.Cz

Nucleon-deuteron elastic scattering at intermediate energies is one of the most promising ways of investigating three-nucleon (3*N*) forces. The differential cross section for such a reaction can be calculated using refined nucleon-nucleon (*NN*) potentials [1–4] and solving the Faddeev equations [5]. By introducing a 3*N* potential—in this case the Tucson-Melbourne force [6]—into the Faddeev equations, it has been shown [7] that the presence of 3*N* forces should appear as a measurable effect in the angular range of the cross-section minimum. Another approach based on chiral perturbation theory (CHPT) gives similar predictions [8].

The effects of 3*N* forces, if present, should be seen in neutron-deuteron (*nd*) as well as in proton-deuteron (*pd*) scattering. Differential cross sections measurements for *pd* elastic scattering are numerous [9–18]. In contrast, there are few *nd* elastic scattering data at intermediate energies. The existing *nd* data sets are at 65 MeV [19], 95 MeV [20], 152 MeV [21], and 250 MeV [22]. At 65 MeV, the data are not able to resolve 3*N* force effects, which are expected to be small at this energy. At 95 and 152 MeV, the data favour the calculations including 3*N* forces. Finally, at 250 MeV, the data reveal an effect which is larger than predicted. At such energies, an ambiguity arises from the fact that relativistic effects are not taken into account by the theoretical descriptions. Thus, *nd* data around 100 MeV are well suited for investigating 3*N* forces: the effect is expected to be about 30% in the minimum region—large enough to be detected—whereas relativistic effects are not expected to contribute significantly.

The present data cover the full angular distribution at 95 MeV, the same energy as the MEDLEY data reported in Ref. [20]. They were obtained with the same neutron beam, and measured by the same research group, but with a completely different experimental setup. The detector setup used this time is SCANDAL (SCAttered Nucleon Detection AssembLy) [23], designed to detect neutrons for elastic scattering cross-section measurements by tracking recoil protons from converter plastic scintillators, with a possibility to remove the converters for detection of protons, and, in our case, also deuterons. One experiment was performed in neutron

*Corresponding author. Telephone: +46 18 471 3788. Email address: jan.blomgren@tsl.uu.se

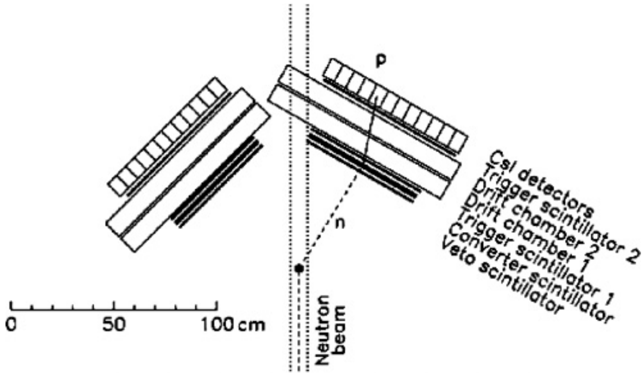

FIG. 1. Schematic layout of the SCANDAL setup [23]. In the present experiment (in neutron detection mode), the converter detector consisted of two plastic scintillators on each arm. A typical event is indicated.

detection mode and covers the angular range 15–100° for the neutron angle in the c.m. system. A second experiment was performed in deuteron detection mode, covering the angular range 105–158°, corresponding to the cross-section minimum.

The neutron beam was produced by the ^{7}Li$(p,n)^7$Be reaction at the neutron beam facility at The Svedberg Laboratory (TSL) in Uppsala before the upgrade of the facility. The high-energy peak in the neutron spectrum had an energy of 94.8 MeV, an FWHM of 2.7 MeV, and a flux of about 4×10^4 n/(cm^2 s) at the target position. The relative neutron fluence was monitored by two independent monitors based on the ^{238}U(n, f) reaction. The SCANDAL setup (see Fig. 1) consists of two identical arms that can be positioned on either side of the beam and rotated around the target position. Each arm can be equipped with a 2 mm thick veto scintillator for charged-particle rejection, two converter scintillators of 20 mm and 10 mm thickness for neutron-proton conversion, a 2 mm thick ΔE plastic scintillator for triggering, two drift chambers (DCH) giving two horizontal and two vertical positions for proton tracking, another 2 mm thick ΔE plastic scintillator for triggering, and an array of 12 CsI detectors. A full description of the SCANDAL setup and the TSL neutron beam facility is presented in Ref. [23].

The plastic scintillators and the CsI crystals were energy-calibrated by detecting recoil protons from *np* scattering at small angles, using the standard SCANDAL calibration procedure described in Ref. [23].

In neutron detection mode, the full setup was used, including veto, thick converter, and thin converter scintillators. The left arm was placed at −58° and the right arm at 32°. As

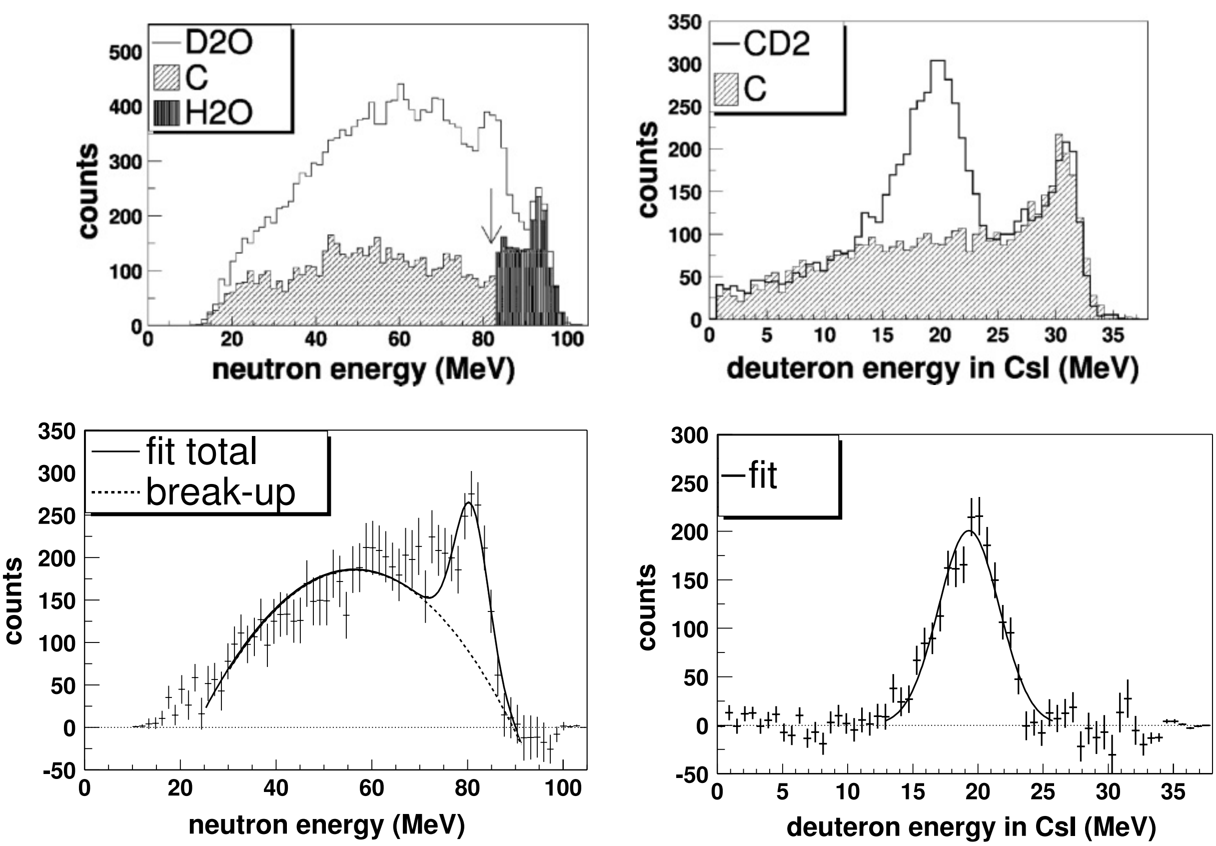

FIG. 2. Typical energy spectra for neutrons detected at 30° (left panels) and for deuterons detected at 32° (right panels). In the top left panel, the instrumental background has been subtracted. The bottom left panel shows the *nd* spectrum after subtraction of the oxygen content in D_2O and the contribution from elastic events converted in carbon (see text), fitted with a second degree polynomial plus a Gaussian in order to account for the deuteron breakup and elastic scattering, respectively. The bottom right panel shows the *nd* elastic peak after subtraction of the carbon content in CD_2 (in deuteron mode, break-up events are rejected by a particle identification cut). The error bars in the bottom panels are due to statistics.

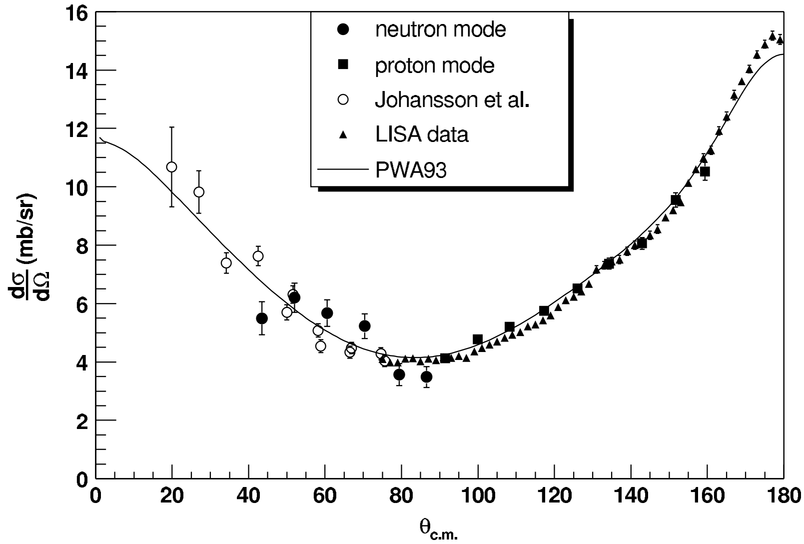

FIG. 3. The *np* differential cross section at 95 MeV. The error bars include both the statistical and systematic uncertainties. In neutron mode (filled circles), the data were normalized to the C(n, n) elastic scattering cross section [26] and can be compared with the Johansson *et al*. data [24] also taken with SCANDAL and normalized to the total *np* cross section. In proton mode (filled squares), the data were normalized to the LISA data [27] (filled triangles). The solid line represents the Nijmegen partial-wave analysis PWA93 [28].

targets, we used water (H_2O) and heavy water (D_2O) contained in cylindrical aluminium cans 8.5 cm in diameter, an empty can (EMPTY) for the instrumental background subtraction, and a graphite target cylinder 8 cm in diameter for normalization purposes. In a first-stage analysis, the data were treated on an event-by-event basis, selecting valid events the same way as described in detail in Ref. [24].

For the 12 angular bins of each arm defined by the 12 CsI crystals, the selected events were projected as neutron energy histograms. The spectra obtained with the H_2O, D_2O and EMPTY targets were normalized to the same neutron fluence—measured with the fission monitors and corrected for dead time. The instrumental background was eliminated by subtracting the EMPTY spectra from the H_2O and D_2O spectra. The oxygen background was canceled by subtracting the H_2O and D_2O spectra from each other, using also spectra from the graphite target [normalized to the same number of elastic events in O(n, n) and C(n, n) scattering] to simulate scattering from oxygen in the low-energy part of the spectra where *nd* and *np* scattering overlap. This is illustrated in the top left panel of Fig. 2, where the arrow indicates the end of the *np* peak, up to which the carbon spectrum is used. Additionnally, not shown in the figure is the subtraction of *nd* elastic events converted in carbon, which gives a contribution up to 10 MeV below the elastic peak [23,24]. The remaining *nd* spectra, as illustrated in the bottom left panel of the figure, were corrected for deuteron breakup by subtracting a second-order polynomian curve which was fitted to the break-up background. All these background subtraction procedures are not straightforward and will be described in more detail in a coming publication [25]. Finally, the elastic peaks were integrated to obtain the number of *np* and *nd* elastic events.

A correction for neutron multiple scattering and attenuation inside the target was applied as described in Ref. [24]. The data were corrected for the fraction of events due to low-energy neutrons, the CsI efficiency and the conversion efficiency, all these effects being slightly angle-dependent. The systematic uncertainty per point was typically $\pm 12\%$ and was heavily dominated by uncertainties in the oxygen and breakup background subtractions [25].

Differential cross sections were obtained for four sets of data: left and right arm with conversion in the thin and thick

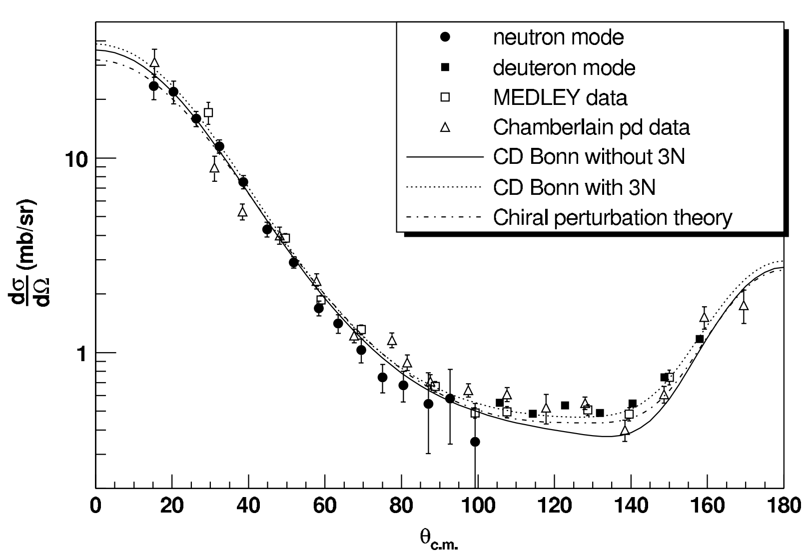

FIG. 4. The *nd* differential cross section at 95 MeV. The error bars include both the statistical and systematic uncertainties. In neutron mode (filled circles), the data were normalized to the C(n, n) elastic scattering cross section [26], and in deuteron mode (filled squares), the data were normalized to the *np* differential cross section (see Fig. 3). The present results are compared with the MEDLEY *nd* data [20] and Chamberlain and Stern *pd* data [10]. The theoretical curves are calculations using the CD-Bonn potential with (dotted line) and without (solid line) $3N$ forces [7], and CHPT calculations [8] (dashed line).

converter. Absolute normalization of these data was made relative to the $^{12}C(n,n)$ total elastic scattering cross section, handling the data from the graphite target the same way as in Ref. [26]. Knowing the total elastic cross section on carbon with an accuracy of $\pm 2.5\%$, as well as the relative neutron fluences and the relative number of nuclei inside the different targets with an accuracy better than $\pm 1\%$, the uncertainty in the normalization with this method was dominated by the quality of the fit to the $C(n,n)$ data and was estimated to be $\pm 4\%$. After normalization, the four sets of data were combined into one single set of data, reducing both the statistical and systematic uncertainties per point. The final *np* data are shown as filled circles in Fig. 3, and the *nd* data in Fig. 4. A good agreement between the present *np* data and the *np* data at the same energy measured by Johansson *et al.* [24]—which were normalized to the total *np* cross section—provides a valuable consistency check of our normalization method.

In deuteron detection mode (proton detection for *np* scattering), the veto and converter scintillators were removed from the SCANDAL arms used one at a time, disposed alternatively at 32° and −32° with respect to the beam. As targets, we used about 1 mm thick CD_2, CH_2 and graphite (C) target foils placed simultaneously inside a multitarget (MTGT) box (described in Ref. [23]). The MTGT multiwire proportional counter information was used to determine in which target the reaction took place. The data were sorted into 12 angular bins (one for each CsI). A time-of-flight criterion was applied to reject the low-energy part of the neutron spectrum. A cut in $\Delta E/E$ two-dimensional plots allowed to distinguish protons from deuterons.

For each angular bin, the remaining events were projected as energy spectra, as illustrated in the top right panel of Fig. 2. The *np* and *nd* peaks were obtained by subtracting the C spectra from the CH_2 and CD_2 spectra (see the bottom right panel of Fig. 2), and were integrated to obtain the number of elastic events.

Corrections were applied for the MTGT efficiency, the CsI efficiency, and the contamination from low-energy neutrons.

TABLE I. The measured *nd* elastic scattering differential cross section at 95 MeV incident neutron energy. In neutron detection mode, the data were normalized to the $C(n,n)$ total elastic scattering cross section [26], and in deuteron mode to the *np* differential cross section [27], in both cases with a normalization uncertainty of $\pm 4\%$. The uncertainty in the neutron c.m. angle is 0.5°.

$\theta_{\mathrm{c.m.}}$ (degrees)	$\frac{d\sigma}{d\Omega}(\frac{mb}{sr})$	$\delta_{\mathrm{stat}}(\frac{mb}{sr})$	$\delta_{\mathrm{sys}}(\frac{mb}{sr})$
Neutron mode			
15.2	24.99	1.07	3.73
20.4	23.33	0.87	3.04
26.3	17.04	0.53	1.45
32.4	12.26	0.42	0.85
38.7	7.91	0.28	0.57
44.8	4.50	0.23	0.35
51.8	3.14	0.13	0.18
58.3	1.86	0.11	0.10
63.5	1.55	0.11	0.09
69.4	1.10	0.09	0.06
75.0	0.85	0.07	0.06
80.5	0.72	0.08	0.04
87.0	0.59	0.19	0.07
92.7	0.62	0.18	0.07
99.3	0.37	0.19	0.04
Deuteron mode			
105.7	0.552	0.010	0.014
114.3	0.484	0.009	0.012
122.8	0.535	0.010	0.013
131.9	0.488	0.010	0.013
140.4	0.548	0.013	0.014
148.8	0.744	0.016	0.019
158.0	1.172	0.025	0.034

The measurements beyond about 45° laboratory angle were discarded due to large energy losses inside the experimental setup. The systematic uncertainty per point was evaluated to typically $\pm 5\%$, due to uncertainties in the solid angle, the event selection and the corrections.

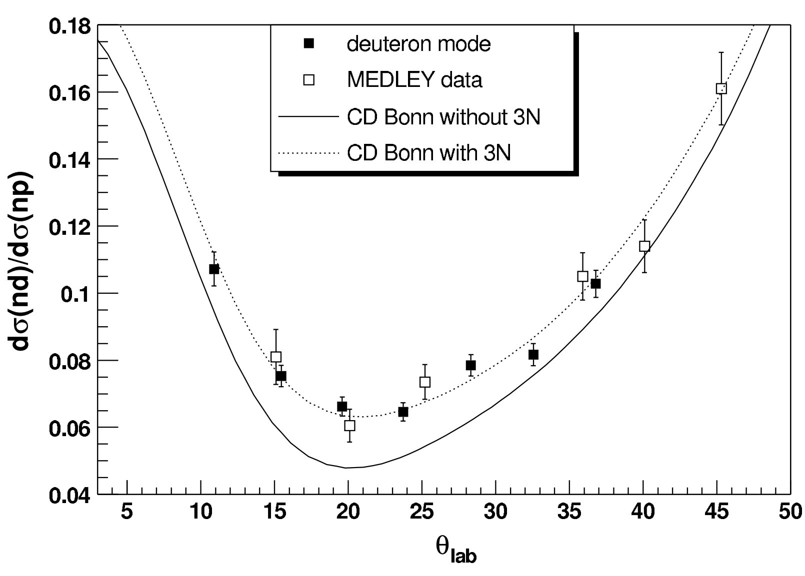

FIG. 5. Ratio of the *nd* cross section to the *np* cross section at 95 MeV in the minimum region, as a function of the detected particle angle in the laboratory. This ratio is independent of normalization uncertainties. The present results (filled squares) are compared with the MEDLEY results [20] (open squares), and with calculations based on the CD-Bonn potential with and without $3N$ forces [3,7].

The four sets of data—left and right arms placed on the left and right side of the beam—were independently normalized to the *np* scattering cross section, minimizing the χ^2 between the present *np* data and the high-quality LISA data [27]. This procedure gave an uncertainty of $\pm 4\%$ in the absolute normalization. Then, the four data sets were combined. The final *np* data are shown as filled squares in Fig. 3 and the *nd* data in Fig. 4 and in Table I, together with the data in neutron detection mode.

The present data are in very good agreement with the MEDLEY data [20] in both the forward and backward angular ranges. In the forward angular range (neutron mode), the data also agree well with the theoretical predictions. The $3N$ forces in this angular range are so weak compared to *NN* forces that the different predictions give very small differences, that cannot be resolved by the data. On the other hand, a comparison between *nd* and *pd* in this angular range could give information about Coulomb force effects, which are expected to be significant at forward angles [29].

At backward angles (deuteron mode), i.e., in the region of the *nd* cross-section minimum, the data agree fairly well with the Faddeev calculations including $3N$ forces with a reduced χ^2 of 3.7, and disagree spectacularly with the Faddeev calculations that do not include $3N$ forces with a reduced χ^2 of 44. In Fig. 5, we have plotted the ratio of the *nd* cross section to the *np* cross section, as a function of the deuteron/proton angle in the laboratory. This ratio has the advantage to be free from normalization uncertainties. Comparison between our data and the theoretical predictions for this ratio using the CD-Bonn potential gives a reduced χ^2 of 0.6 when $3N$ forces are included and 20 when they are not. The fact that the χ^2 is improved when considering the ratio indicates that the deviation is related to the normalization (here, the data were normalized to *np* scattering with an uncertainty of $\pm 4\%$ in the normalization). If we lower the absolute normalization for *nd* scattering by 4%, the χ^2 is reduced to a value close to one, as for the ratio (see Table II).

TABLE II. Reduced χ^2 between our data in deuteron mode and the different theoretical predictions.

	Without $3N$	With $3N$	CHPT
nd (Fig. 4)	44	3.7	18
$nd \cdot 0.96$	33	1.7	10
ratio *nd*/*np* (Fig. 5)	20	0.6	–

In conclusion, we have performed a new measurement of the *nd* scattering angular distribution at 95 MeV. The theoretical prediction based on Faddeev calculations using the CD-Bonn potential with $3N$ forces describes our data very well in the minimum region, while the same calculations without $3N$ forces are significantly off. The rest of the angular range is well described by all the calculations. This result, together with the previous MEDLEY data that observed the same behavior [20], can be interpreted as a strong evidence for $3N$ force effects.

We wish to thank the technical staff of the The Svedberg Laboratory for enthusiastic and skillful assistance. We are very thankful to E. Epelbaum, W. Glöckle, H. Kamada, and H. Witała for contributions concerning the theoretical part. We have appreciated the precious collaboration of K. Hatanaka and N. Kalantar-Nayestanaki. This work was supported by the Swedish Nuclear Fuel and Waste Management Company, the Swedish Nuclear Power Inspectorate, Ringhals AB, the Swedish Defence Research Agency and the Swedish Research Council.

[1] V. G. J. Stoks, R. A. M. Klomp, C. P. F. Terheggen, and J. J. de Swart, Phys. Rev. C **49**, 2950 (1994).
[2] R. B. Wiringa, V. G. J. Stoks, and R. Schiavilla, Phys. Rev. C **51**, 38 (1995).
[3] R. Machleidt, F. Sammarruca, and Y. Song, Phys. Rev. C **53**, R1483 (1996).
[4] R. Machleidt, Phys. Rev. C **63**, 024001 (2001).
[5] W. Glöckle, H. Witała, D. Hüber, H. Kamada, and J. Golak, Phys. Rep. **274**, 107 (1996).
[6] S. A. Coon and W. Glöckle, Phys. Rev. C **23**, 1790 (1981); S. A. Coon, M. D. Scadron, P. C. McNamee, B. R. Barrett, D. W. E. Blatt, and B. H. J. McKellar, Nucl. Phys. **A317**, 242 (1979).
[7] H. Witała, W. Glöckle, D. Hüber, J. Golak, and H. Kamada, Phys. Rev. Lett. **81**, 1183 (1998).
[8] E. Epelbaum, A. Nogga, W. Glöckle, H. Kamada, Ulf.-G. Meissner, and H. Witała, Phys. Rev. C **66**, 064001 (2002).
[9] H. Shimizu *et al.*, Nucl. Phys. **A382**, 242 (1982).
[10] O. Chamberlain and M. O. Stern, Phys. Rev. **94**, 666 (1954).
[11] H. Sakai *et al.*, Phys. Rev. Lett. **84**, 5288 (2000).
[12] G. Igo *et al.*, Nucl. Phys. **A195**, 33 (1972).
[13] H. Postma and R. Wilson, Phys. Rev. **121**, 1229 (1961).
[14] K. Kuroda, A. Michalowicz, and M. Poulet, Nucl. Phys. **88**, 33 (1966).
[15] K. Sekiguchi *et al.*, Phys. Rev. C **65**, 034003 (2002).
[16] K. Ermisch *et al.*, Phys. Rev. C **68**, 051001(R) (2003).
[17] R. E. Adelberger and C. N. Brown, Phys. Rev. D **5**, 2139 (1972).
[18] K. Hatanaka *et al.*, Phys. Rev. C **66**, 044002 (2002).
[19] H. Rühl *et al.*, Nucl. Phys. **A524**, 377 (1991).
[20] P. Mermod *et al.*, Phys. Lett. **B597**, 243 (2004).
[21] J. N. Palmieri, Nucl. Phys. **A188**, 72 (1972).
[22] Y. Maeda, Ph.D. thesis, University of Tokyo (2004), unpublished.
[23] J. Klug *et al.*, Nucl. Instrum. Methods Phys. Res. A **489**, 282 (2002).
[24] C. Johansson *et al.*, Phys. Rev. C **71**, 024002 (2005).
[25] P. Mermod *et al.*, in preparation.
[26] J. Klug *et al.*, Phys. Rev. C **68**, 064605 (2003).
[27] J. Rahm *et al.*, Phys. Rev. C **63**, 044001 (2001).
[28] V. G. J. Stoks, R. A. M. Klomp, M. C. M. Rentmeester, and J. J. de Swart, Phys. Rev. C **48**, 792 (1993).
[29] A. Deltuva, A. C. Fonseca, and P. U. Sauer, Phys. Rev. C **71**, 054005 (2005).